Journal of Alloys and Compounds 542 (2012) 157–163

Contents lists available at SciVerse ScienceDirect

Journal of Alloys and Compounds

journal homepage: www.elsevier.com/locate/jalcom

Optical and magneto-optical properties of $Nd_{0.5}Gd_{0.5}Fe_3(BO_3)_4$ single crystal in the near IR spectral region

A.V. Malakhovskii [a,*], S.L. Gnatchenko [b], I.S. Kachur [b], V.G. Piryatinskaya [b], A.L. Sukhachev [a], I.A. Gudim [a]

[a] L.V. Kirensky Institute of Physics, Siberian Branch of Russian Academy of Sciences, 660036 Krasnoyarsk, Russian Federation
[b] B. Verkin Institute for Low Temperature Physics and Engineering, National Academy of Sciences of Ukraine, 61103 Kharkov, Ukraine

ARTICLE INFO

Article history:
Received 23 May 2012
Received in revised form 10 July 2012
Accepted 11 July 2012
Available online 20 July 2012

Keywords:
Rare earth compounds
Nd^{3+}
Antiferromagnets
Multiferroics
Magnetic circular dichroism
Absorption spectra

ABSTRACT

Polarized optical absorption and magnetic circular dichroism (MCD) spectra of the trigonal multiferroic $Nd_{0.5}Gd_{0.5}Fe_3(BO_3)_4$ were studied in the region of transitions $^4I_{9/2} \rightarrow {}^4F_{3/2}$ and $^4I_{9/2} \rightarrow ({}^4F_{5/2} + {}^2H_{9/2})$ in Nd^{3+} ion. Components of the crystal field splitting of the states were identified with the help of MCD and polarized absorption spectra. Splitting of the Nd^{3+} absorption lines caused by the magnetic ordering were observed. Splitting of Nd^{3+} ground state in Fe-sublattice exchange field was found to be $\sim$9 cm^{-1} at 5.7 K. The Zeeman splitting of some absorption lines in the external magnetic field and changes of the effective Landé factors in the C_3-direction as a result of the corresponding optical transitions were found. Peculiarities in the temperature behavior of the absorption lines connected both with the ground and excited states were revealed. Peculiarities connected with the excited states testify to the local crystal distortions in the excited states.

1. Introduction

The nearest relatives of the crystal under study, $NdFe_3(BO_3)_4$ and $GdFe_3(BO_3)_4$, the same as some other rare earth (RE) ferroborates, refer to multiferroics [1,2], which possess magnetic and electric order simultaneously. The first measurements [3] confirm that the crystal $Nd_{0.5}Gd_{0.5}Fe_3(BO_3)_4$ is also a multiferroic. All RE ferroborates are magnetically ordered at temperatures below 30–40 K. Magnetic ordering of two-component borates $Nd_xGd_{1-x}Fe_3(BO_3)_4$ was studied in [4] by the spectroscopy method. It was found that the increase of Nd concentration results in the decrease of the magnetic ordering temperature as well as of the spin-reorientation temperature. The crystal $Nd_{0.5}Gd_{0.5}Fe_3(BO_3)_4$ becomes antiferromagnetic at T_N = 32 K and preserves easy plane magnetic structure down to 2 K [5]. At temperatures T < 11 K hysteresis in magnetization of the crystal in the easy plane was found that indicated appearance of the static magnetic domains [5]. At room temperature, the crystal has trigonal symmetry with the space group $R32$ and the lattice constants are: a = 9.557(7) Å and c = 7.62(1) Å [5]. The unit cell contains three formula units. Trivalent RE ions occupy D_3 symmetry positions. They are located at the center of trigonal prisms made up of six crystallography equivalent oxygen ions. The triangles formed by the oxygen ions in the neighboring basal planes are not superimposed on each other but are twisted through a particular angle. The FeO_6 octahedrons share edges in such a way that they form helicoidal chains, which run parallel to the C_3 axis and are mutually independent. In the crystal at room temperature, all Fe ions occupy C_2-symmetry positions.

Optical spectra and crystal field parameters of $NdFe_3(BO_3)_4$ were studied in Ref. [6]. Spectroscopic characteristics of $Nd_{0.5}Gd_{0.5}Fe_3(BO_3)_4$ were presented in Ref. [7]. There is a number of works devoted to study of magnetic circular dichroism (MCD) in different materials and in Nd^{3+} containing compounds, in particular (see, e.g. [8–12] and references therein). The MCD gives an additional source of information about properties of electronic states [13] that will be used in the present work for interpretation of the experimental results obtained. The changes of magnetic and electric states of the RE ferroborates, caused both by the phase transitions or by the external fields, substantially influence the parameters of the f–f absorption spectra (e.g. [14–17] and references therein). This is of interest from the viewpoint of applications. There is also possible particular local behavior of the substance in the excited electronic state different from that in the ground state [17,18]. In the present work, on the basis of absorption and MCD spectra, we analyze properties of some $4f$ electronic states of Nd^{3+} ion in the $Nd_{0.5}Gd_{0.5}Fe_3(BO_3)_4$ single crystal and their transformations with the temperature variation.

2. Experimental details

$Nd_{0.5}Gd_{0.5}Fe_3(BO_3)_4$ single crystals were grown from the melt solution on the base of $K_2Mo_3O_{10}$ as described in Ref. [19]. The absorption spectra were measured using diffraction monochromator MDR-23 with diffraction grating 1200 lines/mm and linear dispersion 1.3 nm/mm. The spectral resolution was about 1 cm^{-1} in

* Corresponding author. Tel.: +7 3912 494556; fax: +7 3912 438923.
E-mail address: malakha@iph.krasn.ru (A.V. Malakhovskii).

0925-8388/$ - see front matter © 2012 Elsevier B.V. All rights reserved.
http://dx.doi.org/10.1016/j.jallcom.2012.07.061

the studied spectral region. The spectra were measured with the light propagating normal to the C_3 axis of the crystal for the light electric vector $\vec{E}$ parallel (the π spectrum) and perpendicular (the σ spectrum) to the C_3 axis and the light propagating along the C_3 axis (the α spectrum). The light was polarized by the Glan prism. Precise positions of polarization parallel to the main crystal axes were found according to minimum transparency of the sample in crossed polarizers. The absorption spectra measured in the σ and α polarizations coincide with each other within the limit of the experimental error. This implies that the absorption mainly occurs through the electric dipole mechanism. A liquid-helium cooled cryostat was used for low temperature measurements. It had an internal volume filled by gaseous helium where the sample was placed; the temperature of the sample was regulated by heating element.

MCD was measured using the modulation of the light wave polarization with piezoelectric modulator. The modulator consists of the plate of fused silica and piezoelectric ceramic element pasted to it. The modulator is a part of the self-contained generator and oscillates with its resonance frequency of about 25 kHz. Linearly polarized light passed through the plate of the fused silica changes its polarization from right to left circular one with the resonance frequency of the modulator. The circularly polarized light passed through the sample acquires a modulation of its intensity due to circular dichroism of the sample. At the light wavelength changing, the photomultiplier direct current level is maintained constant due to the feedback controlled high voltage power supply of the photoelectron multiplier. Thus, circular dichroism is proportional to alternating current of the photoelectron multiplier at the frequency of modulation. Calibration of the circular dichroism measurements was fulfilled by the method described in Ref. [20]. MCD was measured as a difference of circular dichroism in plus and minus magnetic field. So, natural circular dichroism, existing in the non centrosymmetrical crystal, was excluded. The MCD spectra were measured automatically with the help of the computer controlled program. Optical slit-width was $\sim$10 cm^{-1}. Magneto-optical measurements were carried out in a magnetic field of 5 kOe. The sample was put in a nitrogen gas flow cryostat. Accuracy of the temperature measuring was $\sim$1 K. MCD measurements were carried out in α-polarization.

3. Results and discussion

Absorption spectra of the $Nd_{0.5}Gd_{0.5}Fe_3(BO_3)_4$ crystal in π and σ polarizations at room temperature are shown in Fig. 1. They consist of narrow bands corresponding to f–f transitions in Nd^{3+} ions and of wide bands due to d–d transitions in Fe^{3+} ions ($^6A_1 \rightarrow {}^4T_1$ and $^6A_1 \rightarrow {}^4T_2$ in cubic crystal field notation). At $E \sim 22900$ cm^{-1} there is a comparatively strong d–d transition $^6A_1 \rightarrow {}^4A_1{}^4E$ and at $E \sim 25000$ cm^{-1} the edge of the strong absorption is observed, which is due to inter-atomic Fe–Fe (Mott–Hubbard) transitions and to charge transfer transitions $2p \rightarrow 3d$ between molecular $2p$-orbitals of ligands and $3d$-orbitals of the Fe^{3+} ion inside FeO_6 cluster. On the first stage the f–f absorption bands were erased from the total spectra. The remained spectra were approximated by the Gauss functions and thus the d–d spectra were obtained separately (Fig. 1). Then the d–d spectra were subtracted from the total spectra and so the f–f spectra were obtained. Identification of the f–f spectra was made according to Ref. [21]. Absorption spectra of transitions $^4I_{9/2} \rightarrow {}^4F_{3/2}$ (R-band) and $^4I_{9/2} \rightarrow {}^4F_{5/2} + {}^2H_{9/2}$ (S-band) in Nd^{3+} ions were studied in the temperature range of 5.7–300 K and MCD spectra in the temperature range of 90–300 K. Symbols R and S were given according to Ref. [22]. Absorption spectra of these transitions are presented in Figs. 2–4.

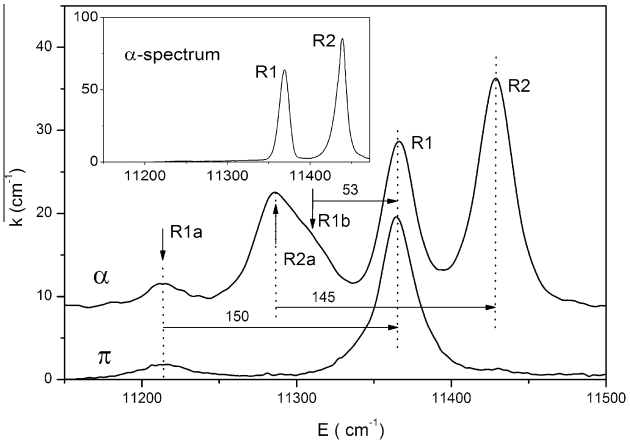

Fig. 2. π and α absorption spectra of the $^4I_{9/2} \rightarrow {}^4F_{3/2}$ transition (R-band) in Nd^{3+} ions at T = 90 K. Insert – α spectrum at T = 5.7 K.

Let us consider the transition $^4I_{9/2} \rightarrow {}^4F_{3/2}$ (Fig. 2). All states with the half integer total moments are split in the crystal field of D_3 symmetry into the Kramers doublets (see Table 1). If one supposes that the lowest level is $E_{3/2}$, then, according to the selection rules (Table 1), only one absorption line in $\alpha(\sigma)$-polarization should be observed at low temperature, in contrast to the experiment (Fig. 2, Inset). Thus, the symmetry of the lowest level of the ground multiplet ($Gr1$) is $E_{1/2}$ and the symmetries of the levels $R1$ and $R2$ are $E_{1/2}$ and $E_{3/2}$, respectively (Table 2). The lines $R1a$ and $R2a$ correspond to the transitions from the level $Gr3$ at the energy $\sim$150 cm^{-1} (Fig. 2, Table 2). They have the same linear polarizations as the lines $R1$ and $R2$ have. Therefore, the level $Gr3$ is of $E_{1/2}$ symmetry. The line $R1b$ can be referred to the transition from the $Gr2$-level of $E_{3/2}$ symmetry (Table 2), since it is observed only in $\alpha(\sigma)$ polarization (Fig. 2). Similarly, from the line polarizations (Figs. 3 and 4) and with the help of selection rules of Table 1, the symmetry of states in the S-manifold was found (see Table 2). The line $S2a$ should present in principle in π-polarization, but probably it is too weak. Position of the level $Gr3$ is a little different, when we find it relative to the level $R1$ or to the level $R2$ (Fig. 2). It

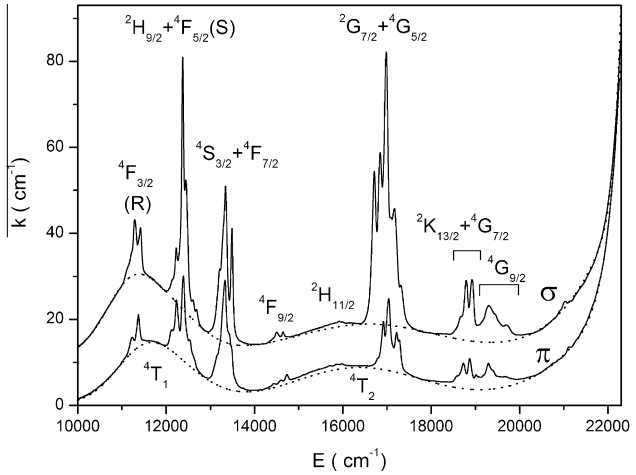

Fig. 1. π and σ absorption spectra of the $Nd_{0.5}Gd_{0.5}Fe_3(BO_3)_4$ single crystal at room temperature. Dotted lines correspond to d–d transition spectra of Fe^{3+} ion.

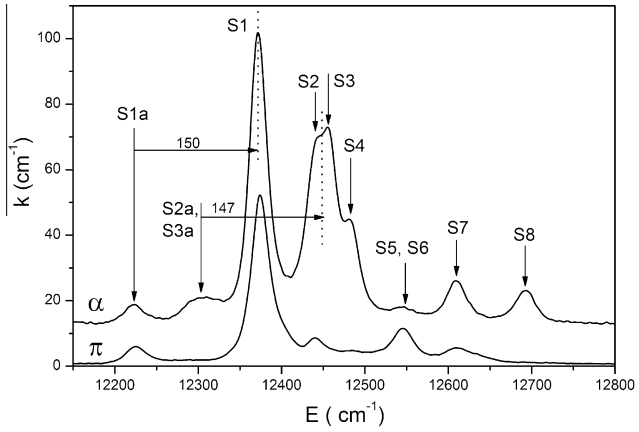

Fig. 3. π and α absorption spectra of the $^4I_{9/2} \rightarrow {}^4F_{5/2} + {}^2H_{9/2}$ transition (S-band) in Nd^{3+} ions at T = 90 K.

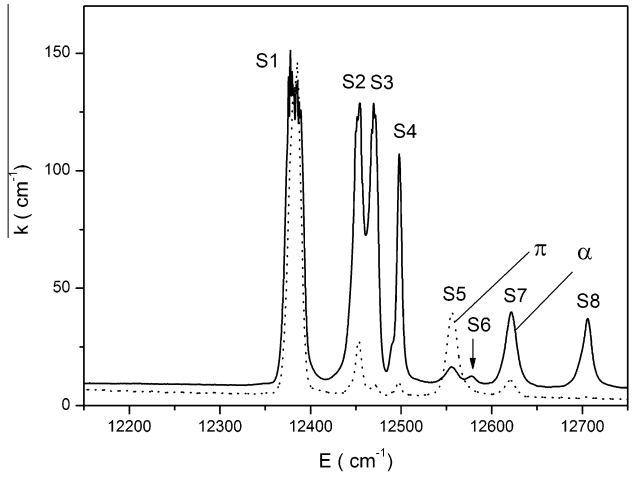

Fig. 4. π and α absorption spectra of the $^4I_{9/2} \rightarrow {}^4F_{5/2} + {}^2H_{9/2}$ transition (S-band) in Nd^{3+} ions at $T = 5.7$ K.

Table 1
Selection rules for electric dipole transitions in D_3 symmetry.

	$E_{1/2}$	$E_{3/2}$
$E_{1/2}$	π, $\sigma(\alpha)$	$\sigma(\alpha)$
$E_{3/2}$	$\sigma(\alpha)$	π

could be also said that the distance between states *R*1 and *R*2 is different when it is measured, observing from the state *Gr*1 or *Gr*3. That is, the result depends on the states involved in the transitions.

The lines *R*2, *S*2, *S*3, *S*4 and *S*8 reveal splitting in the process of the magnetic ordering. The positions of the splitting components were found from the second energy derivatives of the spectra, since it is more precise. Temperature dependences of some splitting component positions are shown in Figs. 5–7 and values of the splitting at $T = 5.7$ K are given in Table 2. It is necessary to take into account that magnetic moments of the studied crystal sublattices are in the basis plane perpendicular to the C_3 axis [5]. Therefore, observed splitting is due to the effective exchange field H_e of the Fe-sublattice in this plane and is equal to:

$$\Delta E_{ex} = \mu_B(g_{\perp i}H_{ei} - g_{\perp f}H_{ef}) \quad (1)$$

Indexes *i* and *f* refer to initial and final states, respectively. All the enumerated above transitions (except *S*4) have excited states with the theoretical $g_\perp = 0$ or close to zero in the similar crystal $NdFe_3(BO_3)_4$ (see Ref. [6] and Table 1). Therefore the observed splitting of lines are due only to the exchange splitting of the ground state. Assuming the observed differences between the splitting values as being result of the experimental error, we find the average splitting of the ground state of Nd^{3+} ion in the exchange field of the Fe-sublattice in the basis plane: $\Delta E_{ex} = 9.0$ cm^{-1}. All temperature dependences of the splitting components positions reveal asymmetry relative to the line positions at T_N (e.g. Figs. 5–7). This testifies to a relative shift of the states due to the magnetic ordering. There are singularities in the temperature dependences of *R*2 and *S*8 line positions at 16 and 14 K, respectively (Figs. 5 and 7). Probably, these singularities are connected with appearance of domains at 12 K [5]. Difference of the singularities temperatures and the temperature of the domains formation is connected with the change of the local properties of the crystal in the excited state.

Figs. 8 and 9 present temperature dependences of intensities of some absorption lines. The intensities of all transitions beginning from the same state (the ground state, in particular) should have identical temperature dependences governed by the thermal population of the initial state. This is approximately valid for lines of the *S*-band (Fig. 9). Another situation occurs in the *R*-band (Fig. 8). First, the temperature dependences of intensities of the *R*1 line in π- and α-polarizations are substantially different. This testifies to local temperature dependent crystal distortions just in the *R*1 excited state. Second, there are two singularities (increases): in the region of $T = T_N$ for the *R*1-line and at $T = 16$ K both for the *R*1- and *R*2-lines that means increase of the local distortions in the regions of T_N and temperature of the domain formation [5]. All these features are connected with the local properties in the excited states, since similar features are not observed in the *S*-band (Fig. 9).

Temperature dependences of widths of some absorption lines are depicted in Figs. 10 and 11. All they reveal increase of the line-widths in the region of $T \sim 16$ K. There are two possible sources of the electron absorption line broadening: the homogeneous broadening of different nature (anharmonicity of vibrations, change of elastic constants during the electron transition, nonradiative electron–phonon relaxation and so on) and inhomogeneous broadening. The latter is more probable, since in this temperature range the magnetic domains and domain walls appear: [5]. Domain walls are the main source of the crystal inhomogeneity. However, there is also possible virtual broadening due to a small exchange splitting not visible directly.

MCD spectra of the studied bands at temperature of 90 K are shown in Figs. 12 and 13. They permit to obtain additional information about the electronic states involved into transitions. The MCD conditioned by a pair of the Zeeman splitting components is evidently described by the equation:

Table 2
Parameters of transitions and states (details are in the text). Energies of transitions (E) are given at 40 K.

State	Level	E cm^{-1}	Pol.	Sym.	μ	$\Delta\omega_0$	m	Δg_C (exp)	ΔE_{ex} cm^{-1}	$g_\perp$ [6]	g_C [6]	$g_{C\max}$
$^4I_{9/2}$	*Gr*1	0	–	$E_{1/2}$	$\mp$1/2	–	±5/2	–	–	2.385	1.376	3.64
	*Gr*2	53	–	$E_{3/2}$	3/2	–	±9/2	–	–	0	3.947	6.54
	*Gr*3	150	–	$E_{1/2}$	±1/2	–	±7/2	–	–	2.283	2.786	5.09
$^4F_{3/2}$	*R*1	11369	π, σ	$E_{1/2}$	±1/2	(+)	±1/2		~0	0.926	0.251	0.4
	*R*2	11436	σ	$E_{3/2}$	3/2	(−)	±3/2	-0.3	10	0	1.562	1.2
$^4F_{5/2}$	*S*1	12382	π, σ	$E_{1/2}$	±1/2	(−)	±1/2			3.158	0.598	1.03
	*S*2	12450	π, σ	$E_{1/2}$	$\mp$1/2	(+)	±5/2		9.6	0.096	4.713	5.14
	*S*3	12467	σ	$E_{3/2}$	3/2	(+)	±3/2		7.8	0	2.576	3.09
$^2H_{9/2}$	*S*4	12495	π, σ	$E_{1/2}$	±1/2	(−)	±1/2		9.0	3.995	0.982	0.909
	*S*5	12553	π, σ	$E_{1/2}$	±1/2		±7/2		~0	1.989	4.633	6.36
	*S*6	12578	σ	$E_{3/2}$	3/2		±3/2			0	2.169	2.73
	*S*7	12620	π, σ	$E_{1/2}$	$\mp$1/2	(+)	±5/2	+2.8	~0	2.877	2.765	4.55
	*S*8	12702	σ	$E_{3/2}$	3/2	(+)	±9/2	+8.6	8.8	0	7.788	8.18

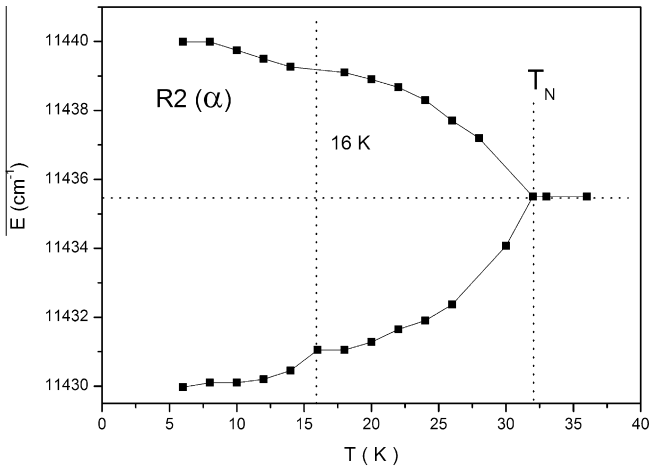

Fig. 5. Splitting of the *R2*-line in α polarization as a function of temperature.

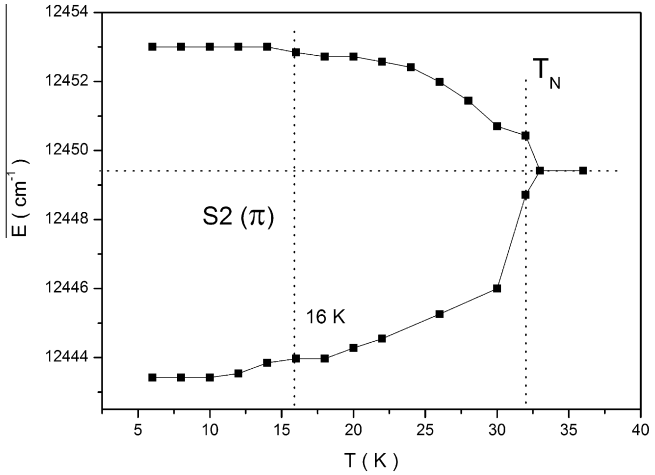

Fig. 6. Splitting of the *S2*-line in π polarization as a function of temperature.

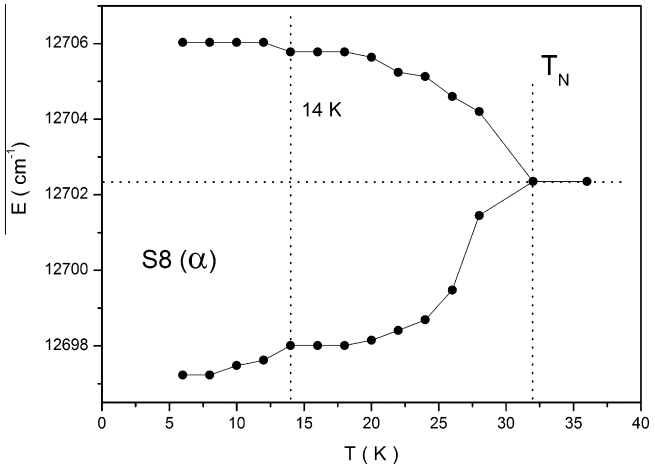

Fig. 7. Splitting of the *S8*-line in α polarization as a function of temperature.

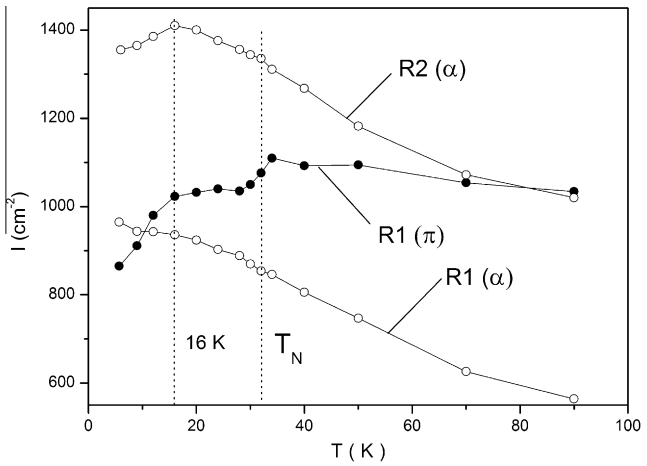

Fig. 8. Intensities of absorption lines as a function of temperature.

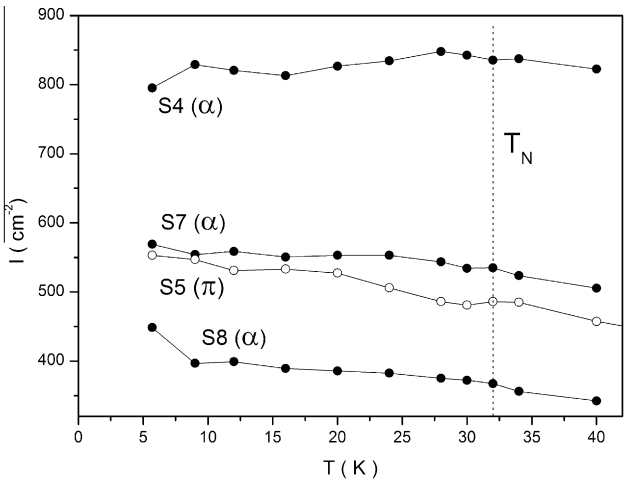

Fig. 9. Intensities of absorption lines as a function of temperature.

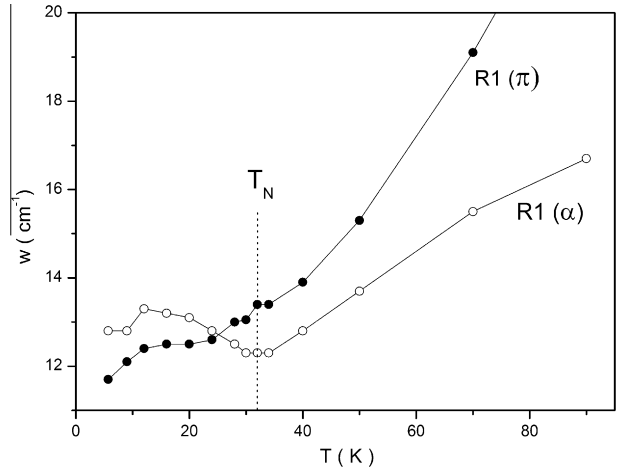

Fig. 10. Line widths as a function of temperature.

$$\Delta k = k_{m+}\varphi(\omega, \omega_0 + \Delta\omega_0) - k_{m-}\varphi(\omega, \omega_0 - \Delta\omega_0) \quad (2)$$

Here k_+ and k_- are amplitudes of (+) and (−) circularly polarized lines; φ are form functions of (+) and (−) lines. In majority of cases, the (−) polarized line has higher frequency ($\Delta\omega_0$ is negative). Signs of $\Delta\omega_0$ in Figs. 12 and 13 and in Table 2 are shown according to definition (2). If the Zeeman splitting $\Delta\omega_0$ is much less than the line width then, developing the form functions as series in $\Delta\omega_0$, one obtains

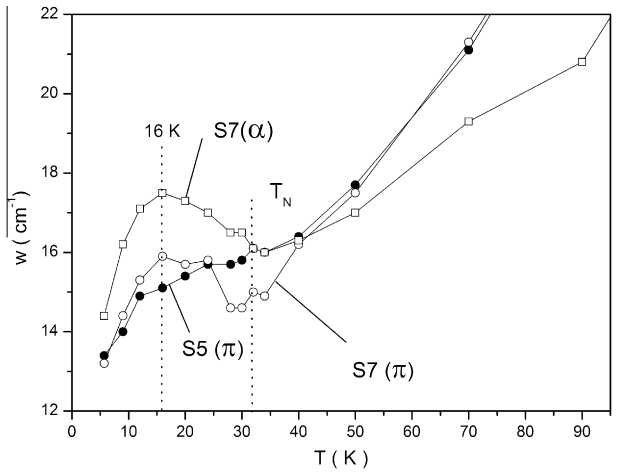

Fig. 11. Line widths as a function of temperature.

$$\Delta k = k_m c\varphi(\omega,\omega_0) + k_m \Delta\omega_0 \partial\varphi(\omega,\omega_0)/\partial\omega_0. \quad (3)$$

Here $k_m = k_{m+} + k_{m-}$ is amplitude of the line not split by the magnetic field and $c = (k_{m+} - k_{m-})/k_m$. The first term in (3) is the paramagnetic temperature dependent MCD and the second one is the diamagnetic effect independent of temperature. The Zeeman splitting of an absorption line $2\Delta\omega_0$ is found through the Zeeman splitting of the initial and final levels:

$$2\hbar\Delta\omega_0 = \pm(\Delta E_i \pm \Delta E_f). \quad (4)$$

The splitting of the Kramers doublets in a magnetic field directed along the C_3 axis of a crystal is represented in the form:

$$\Delta E = \mu_B g_c H, \quad (5)$$

where g_C is the effective Landé factor in the C-direction. Therefore

$$2\bar{h}\Delta\omega_0 = \mu_B H \Delta g_c. \quad (6)$$

The fine structure of the MCD spectra (Figs. 12 and 13) is due to the diamagnetic effect. Sign of the temperature dependent paramagnetic effect (c) is defined by polarization of the transition from the lower component of the Zeeman splitting of the initial state. Sign of the diamagnetic effect ($\Delta\omega_0$) is not so unambiguous. The first sign in (4) refers to the sign of the paramagnetic effect and the second one shows that the splitting of states can sum up and

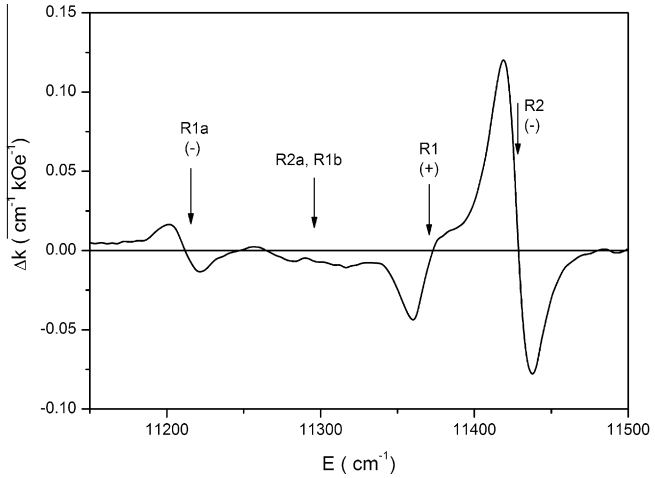

Fig. 12. MCD spectrum of the $^4I_{9/2} \rightarrow {}^4F_{3/2}$ transition (R-band) in Nd^{3+} ions at T = 90 K.

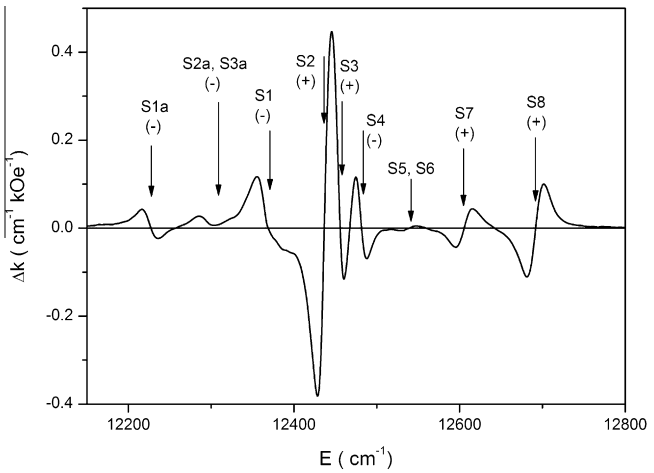

Fig. 13. MCD spectrum of the $^4I_{9/2} \rightarrow {}^4F_{5/2} + {}^2H_{9/2}$ transition (S-band) in Nd^{3+} ions at T = 90 K.

subtract (see below). The experimental signs of the diamagnetic effects of the absorption lines (signs of $\Delta\omega_0$) were found according to definition (2) (see Figs. 12 and 13).

Let us assume that absorption lines in (2) have the Gaussian shape: $\varphi_\pm = \exp\lfloor -(\omega - \omega_0 \pm \Delta\omega_0)^2/2\sigma^2 \rfloor$, where σ characterizes the width of the absorption line (it is the half width at the level $\sqrt{e}$ = 0.606 of the maximum). Then in the same approximation, as the eq. (3) was obtained ($\Delta\omega_0 << \sigma$), we have

$$\Delta\omega_0 = \langle \Delta k(\omega)\rangle_1 / \langle k(\omega)\rangle_0. \quad (7)$$

The first moment is calculated relative to ω_0 and is equal to zero for the paramagnetic effect. The zero moment is equal to zero for the diamagnetic effect and the paramagnetic magneto-optical activity (MOA) is

$$c = \langle \Delta k(\omega)\rangle_0 / \langle k(\omega)\rangle_0. \quad (8)$$

Eq. (8) gives integral paramagnetic MOA for any complicated absorption band, while (7) is, evidently, valid only for one pair of the Zeeman splitting components. It is more convenient to find the Zeeman splitting through values (Δk_{dm}) and positions (ω_m) of extremums of the diamagnetic effect. For the Gaussian $|\omega_m - \omega_0| \approx \sigma$ and

$$\Delta\omega_0 = \frac{\Delta k_{dm}}{k_m} |\omega_m - \omega_0| \sqrt{e}. \quad (9)$$

In the case of the Lorentzian form function, $\sqrt{e}$ should be replaced by "2". If the paramagnetic effect $c << 1$, then the mentioned parameters of the diamagnetic spectrum coincide with those of the total MCD spectrum of the absorption line. Thus, from the parameters of absorption and MCD spectra one can find the Zeeman splitting of the absorption lines and corresponding differences of the effective Landé factor g_C of states according to (6). We have managed to measure splitting of lines $R2$, $S7$ and $S8$ which possess Lorentzian shape (see Table 2). Values Δk_{dm} were found as the half sum of positive and negative extremums. Taking into account the theoretical values of g_C in $NdFe_3(BO_3)_4$ (Table 2), one can say that for $R2$: $\Delta g_C = g_{Ci} - g_{Cf}$, while for $S7$ and $S8$: $\Delta g_C = g_{Ci} + g_{Cf}$.

If a crystal has axis of symmetry, the crystal quantum number, μ, appears. It is an analog of the magnetic quantum number m of a free atom. In the case of C_3 axis and half integer total moment, there are three possible values of the crystal quantum number [23]: μ = + 1/2, −1/2, 3/2 (±3/2). States with $m = \mu \pm 3n$ (where

Table 3
Maximum possible effective Landé factors of states along C_3 axis of a crystal.

	m	9/2	7/2	5/2	3/2	1/2
$^4I_{9/2}$, $g = 0.727$	g_{Cmax}	6.54	5.09	3.64	2.18	0.727
$^4F_{3/2}$, $g = 0.4$	g_{Cmax}				1.2	0.4
$^4F_{5/2}$, $g = 1.029$	g_{Cmax}			5.14	3.09	1.03
$^2H_{9/2}$, $g = 0.909$	g_{Cmax}	8.18	6.36	4.55	2.73	0.909

$n = 0, 1, 2$, etc.) correspond to each μ in the trigonal symmetry [23]. As a result, the following set of states is obtained:

$$m = \pm 1/2, \pm 3/2, \pm 5/2, \pm 7/2, \pm 9/2,$$
$$\mu = \pm 1/2, (\pm 3/2), \mp 1/2, \pm 1/2, (\pm 3/2). \quad (10)$$

States with $\mu = \pm 1/2$ correspond to states $E_{1/2}$ and states with $\mu = (\pm 3/2)$ correspond to states $E_{3/2}$ in the D_3 group notations. In crystals, selection rules for the polarized light absorption are governed by the number μ and they coincide with those for the number m in a free atom [23]:

$$\Delta\mu = \pm 1 \text{ corresponds to } \mp \text{ circularly polarized and } \sigma - \text{polarized waves},$$
$$\Delta\mu = 0 \text{ corresponds to } \pi - \text{polarized waves}. \quad (11)$$

In a homogeneous electric field ($C_{\infty v}$ symmetry), atomic states are split according to the absolute value of magnetic quantum number m. If the atom is also in a magnetic field directed along the homogeneous electric field, each of states with the quantum number $\pm m$ is split. The value of the splitting is

$$\Delta E = 2g\mu_B mH \quad (12)$$

under the condition, that this splitting is much less than the splitting in the electric field. Here g is the Landé factor of the free atom. Eq. (12) can be applied also in the case of the axially symmetric crystal field with m_{eff} instead of m, because states (10) contain admixtures of states with different m. It is so because the matrix of crystal field in the basis of the free atom functions is not diagonal over m in the trigonal symmetry. According to (12) one can estimate maximum possible values of splitting in magnetic field along C_3 axis and according (5) one can find maximum possible values of g_C

$$g_{cmax} = 2gm \quad (13)$$

for all doublets of the ground and excited multiplets of Nd^{3+} ion (Table 3). With the help of (10) and (11), and taking into account splitting (12) in magnetic field according to m, but not according to μ, the diagrams of transitions and their polarizations in magnetic field directed along the C_3 axis can be created (see Fig. 14). Transitions from the levels $m = 7/2$ and $5/2$ of the ground multiplet differ by signs of the polarization according to (10) and (11). As it was said above, sign of the paramagnetic MCD (c) is unambiguously defined by polarization of transition from the lower component of the Zeeman splitting, but sign of the diamagnetic MCD ($\Delta\omega_0$) depends also on the sign in brackets in eq. (4), i.e., on the correlation between splitting (the effective Landé factors) of the initial and final states. In the first approximation we supposed that, according to (13), g_C is proportional to m. When the splitting of a line is equal to the difference of the splitting of the states (sign minus in (4) in brackets), the sign of the line splitting is under the question (Fig. 14).

Let us consider the transition $^4I_{9/2} \rightarrow {}^4F_{3/2}$ (Figs. 2 and 12). As it was found above, the symmetry of the lowest level is $E_{1/2}$. There are at least two suitable levels with such symmetry: $m = \pm 7/2$ ($\mu = \pm 1/2$) and $m = \pm 5/2$ ($\mu = \mp 1/2$) (Fig. 14). However, according to Fig. 14, only in the case of the ground state $m = \pm 5/2$ ($\mu = \mp 1/2$) diamagnetic MCD of lines $R1$ and $R2$ has experimentally observed signs (Fig. 12). Despite the trigonal symmetry of the $Nd_{0.5}Gd_{0.5}Fe_3(BO_3)_4$ crystal, it has easy plane magnetic anisotropy [5], i.e., crystallographic single axial anisotropy is not strong. As a consequence, the order of levels and their Landé factors can not correspond to value of the magnetic quantum number m of the free atom. The lines $R1a$ and $R2a$ can be referred to the transitions from the level $m = \pm 7/2$ ($\mu = \pm 1/2$) at the energy $\sim$150 cm^{-1} and the line $R1b$ – to the only allowed in the σ-polarization transition from the level $m = 9/2$, $\mu = 3/2$ (Figs. 2) at the energy 53 cm^{-1} (π-polarized transition $E_{3/2}$–$E_{3/2}$ is not observed). Indeed, according to Fig. 14, transitions from the level $m = 7/2$ should have opposite circular polarizations relative to those of the transitions from the level $m = 5/2$, and the line $R1a$ should have negative diamagnetic MCD ($\Delta\omega_0 < 0$), that is really observed (Fig. 12). The line $R2a$ should have positive diamagnetic effect while the line $R1b$ should have the negative effect, if it is transition from the state $m = 9/2$ ($\mu = 3/2$) (Fig. 14). These lines are close to each other and therefore their MCD compensate each other (see Fig. 12).

Symmetries of states in the S-manifold are found according to the linear polarizations of the absorption lines (Fig. 4), but the genetic origination of the crystal field states from the m-states of the free atom on the ground of the diamagnetic MCD signs is not unambiguous for this manifold. According to the diagram of Fig. 14, the transitions $E_{1/2}$ ($m = 5/2$) → $E_{3/2}$ (S_3, S_6 and S_8 lines)

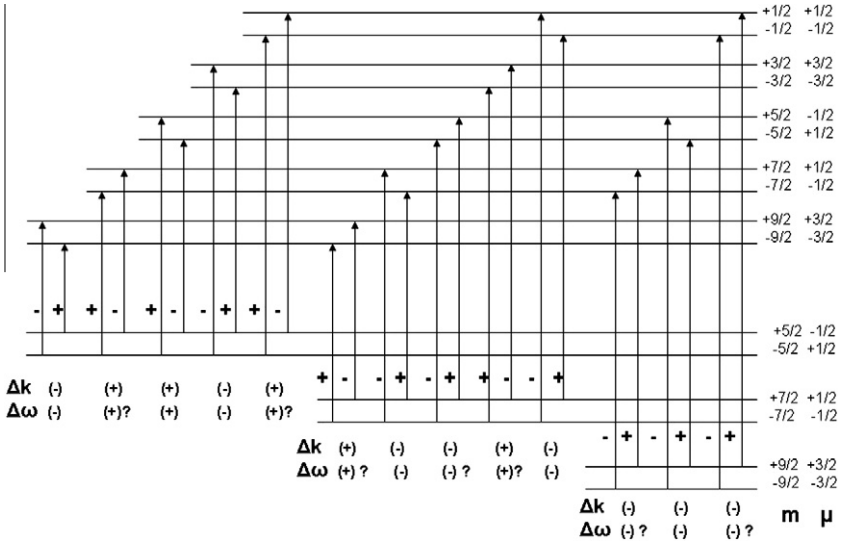

Fig. 14. Diagram of f–f transitions in Nd^{3+} ion.

can have only negative signs of the diamagnetic MCD contrary to the observed ones. Additionally, the lines $S1a$ and $S1$ should have opposite signs of the diamagnetic effect, the same as it takes place for $R1a$ and $R1$ lines (see above). However, the lines $S1a$ and $S1$ have diamagnetic effects of the same sign (Fig. 13). There are two possible origins of the mentioned peculiarities in MCD of the S-band. If we neglect mixing of multiplets by the crystal field, the R-states ($^4F_{3/2}$) are pure m_J states. Another situation takes place in the case of S-states. They are mixing of the m_J states. In particular, according to (10) for the $^4F_{5/2}$ manifold:

$$|E_{1/2}\rangle = a\left|\pm\tfrac{1}{2}\right\rangle + b\left|\mp\tfrac{5}{2}\right\rangle, \quad |E_{3/2}\rangle = \left|\pm\tfrac{3}{2}\right\rangle \tag{14}$$

and for $^2H_{9/2}$:

$$|E_{1/2}\rangle = A\left|\pm\frac{1}{2}\right\rangle + B\left|\mp\frac{5}{2}\right\rangle + C\left|\pm\frac{7}{2}\right\rangle, \qquad |E_{3/2}\rangle = A_1\left|\pm\frac{3}{2}\right\rangle + B_1\left|\pm\frac{9}{2}\right\rangle. \tag{15}$$

The second source of the peculiarities in MCD of the S-band is, probably, the mixing of the close states $^2H_{9/2}$ and $^4F_{5/2}$ composing the S-band. The prevailing m_J-states of the free atom in the crystal field states of the S-manifold can be found basing on the comparison of the maximum possible effective Landé factors $g_{C\max}$ with the theoretical g_C in the $NdFe_3(BO_3)_4$ crystal (Tables 2 and 3). They are of course different but succession of values permits to identify S-states and to confirm identification of the ground ($Gr1$–$Gr3$) and R-states made above (see Table 2). By the way, the theoretical values of g_C for $R2$ and $S4$ states in the crystal appeared to be larger than the maximum possible ones (Table 2). This is rather strange, especially for $R2$-state, since in this multiplet there are no states with larger value of $g_{C\max}$ that could be admixed.

4. Summary

Polarized optical absorption and magnetic circular dichroism (MCD) spectra of the trigonal multiferroic $Nd_{0.5}Gd_{0.5}Fe_3(BO_3)_4$ were studied in the region of transitions $^4I_{9/2} \rightarrow {}^4F_{3/2}$ and $^4I_{9/2} \rightarrow (^4F_{5/2} + {}^2H_{9/2})$ in Nd^{3+} ion. Components of the crystal field splitting of the states were identified with the help of MCD and polarized absorption spectra. In particular, their genetic origin from atomic m_J states was found. Splitting of the Nd^{3+} absorption lines caused by the magnetic ordering were observed. Splitting of Nd^{3+} ground state in the Fe-sublattice exchange field in the basis plane was found to be $\sim$9 cm^{-1} at 5.7 K. The Zeeman splitting of some absorption lines in the external magnetic field and changes of the effective Landé factors in the C-direction as a result of the corresponding transitions were found with the help of the MCD spectra. Peculiarities in temperature behavior of the splitting, intensity and width of the absorption lines were revealed. Features at T = 14–16 K in the temperature dependences of the splitting and intensity of the lines are, probably, connected with the domain formation, locally modified in the excited states. Features in the temperature dependences of the line widths can be due to domain formation and (or) to small exchange splitting not visible directly. Substantial difference of the $R1$-line intensity temperature dependences in two polarizations testifies to local distortions in the $R1$ excited state.

Acknowledgements

The work was supported by the Russian Foundation for Basic Researches Grant 12-02-00026 and by the Russian President Grant SS-1044.2012.2.

References

[1] A.K. Zvezdin, S.S. Krotov, A.M. Kadomtseva, G.P. Vorob'ev, Y.F. Popov, A.P. Pyatakov, L.N. Bezmaternykh, E.A. Popova, Pis'ma v ZhETF 81 (2005) 335. JETP Lett. 81 (2005) 272.
[2] A.K. Zvezdin, G.P. Vorob'ev, A.M. Kadomtseva, Yu.F. Popov, A.P. Pyatakov, L.N. Bezmaternykh, A.V. Kuvardin, E.A. Popova, Pis'ma v ZhETF 83 (2006) 600. JETP Lett. 83 (2006) 509.
[3] A.M. Kadomtseva, Yu.F. Popov, G.P. Vorob'ev, A.A. Mukhin, V.Yu. Ivanov, A.M. Kuz'menko, A.S. Prokhorov, L.N. Bezmaternykh, V.L. Temerov, I.A. Gudim, in: Proceedings of the XXI International Conference "New in Magnetism and Magnetic Materials," Moscow, 2009, p. 316.
[4] E.P. Chukalina, L.N. Bezmaternykh, Fizika Tverdogo Tela 47 (2005) 1470. Physics of the Solid State, 47 (2005) 1528.
[5] A.V. Malakhovskii, E.V. Eremin, D.A. Velikanov, A.V. Kartashev, A.D. Vasil'ev, I.A. Gudim, Fiz. Tverd. Tela 53 (2011) 1929. Phys. Solid State 53 (2011) 2032.
[6] M.N. Popova, E.P. Chukalina, T.N. Stanislavchuk, B.Z. Malkin, A.R. Zakirov, E. Antic-Fidancev, E.A. Popova, L.N. Bezmaternykh, V.L. Temerov, Phys. Rev. B 75 (2007) 224435.
[7] A.V. Malakhovskii, A.L. Sukhachev, A.A. Leont'ev, I.A. Gudim, A.S. Krylov, A.S. Aleksandrovsky, J. Alloys Compd. 529 (2012) 38.
[8] S.J. Collocott, K.N.R. Taylor, J. Phys. C: Solid State Phys. 13 (1979) 3473.
[9] L. Fluyt, I. Couwenberg, H. Lambaerts, K. Binnemans, C. Görller-Walrand, M.F. Reid, J. Chem. Phys. 105 (1996) 6117.
[10] L. Fluyt, E. Hens, H. De Leebeeck, C. Görller-Walrand, J. Alloys Compd. 250 (1997) 316.
[11] H. De Leebeeck, K. Binnemans, C. Görller-Walrand, J. Alloys Compd. 291 (1999) 300.
[12] C. Bonardi, R.A. Carvalho, H.C. Basso, M.C. Terrile, G.K. Cruz, L.E. Bausa, J. Garcia Sole, J. Chem. Phys. 111 (1999) 6042.
[13] C. Görller-Walrand, L. Fluyt, Handbook on the Physics and Chemistry of Rare earths V40 (2010) 2–107.
[14] M.N. Popova, E.P. Chukalina, T.N. Stanislavchuk, L.N. Bezmaternykh, JMMM 300 (2006) e440.
[15] M.N. Popova, T. N Stanislavchuk, B.Z. Malkin, L.N. Bezmaternykh, Phys. Rev. B 80 (2009) 195101.
[16] E.P. Chukalina, M.N. Popova, L.N. Bezmaternykh, I.A. Gudim, Phys. Lett. A 374 (2010) 1790.
[17] A.V. Malakhovskii, S.L. Gnatchenko, I.S. Kachur, V.G. Piryatinskaya, A.L. Sukhachev, V.L. Temerov, Eur. Phys. J. B 80 (2011) 1.
[18] A.V. Malakhovskii, A.L. Sukhachev, S.L. Gnatchenko, I.S. Kachur, V.G. Piryatinskaya, V.L. Temerov, A.S. Krylov, I.S. Edelman, J. Alloys Compd. 476 (2009) 64.
[19] A.D. Balaev, L.N. Bezmaternykh, I.A. Gudim, V.L. Temerov, S.G. Ovchinnikov, S.A. Kharlamova, J. Magn. Magn. Mater. 258-259 (2003) 532.
[20] G.K. Kostyuck, E.K. Galanov, M.V. Leykin, Optiko-mehanicheskaya promishlennost'. 5 (1976) 28. in Russian.
[21] W.T. Carnall, P.R. Fields, B.G. Wybourne, J. Chem. Phys. 42 (1965) 3797.
[22] G.H. Dieke, Spectra and Energy Levels of Rare Earth Ions in Crystals, Interscience Publishers, New York, London, Sydney, Toronto, 1968.
[23] M.A. El'yashevitch. Spectra of rear earths, Moskow, 1953 (in Russian).